Correlation Between Anterior-Posterior and Lateral Dimensions and the Effective and Water-Equivalent Diameters in Axial Images from Head Computed Tomography Examinations

by Eko Hidayanto

Submission date: 12-May-2022 08:10AM (UTC+0700)
Submission ID: 1834229387
File name: C4.pdf (986.62K)
Word count: 4981
Character count: 23684

Radiation Protection Dosimetry (2021), Vol. 196, No. 3–4, pp. 248–256
Advance Access publication 27 September 2021
https://doi.org/10.1093/rpd/ncab144

Note

CORRELATION BETWEEN ANTERIOR–POSTERIOR AND LATERAL DIMENSIONS WITH THE EFFECTIVE AND WATER-EQUIVALENT DIAMETERS IN AXIAL IMAGES FROM HEAD COMPUTED TOMOGRAPHY EXAMINATIONS

Winda Kusuma Dewi[1], Choirul Anam[1,*], Eko Hidayanto[1], Annisa Lidia Wati[1] and Geoff Dougherty[2]
[1]Department of Physics, Faculty of Sciences and Mathematics, Diponegoro University, Semarang, Central Java, Indonesia
[2]Department of Applied Physics and Medical Imaging, California State University Channel Islands, Camarillo, CA 93012, USA

*Corresponding author: anam@fisika.fsm.undip.ac.id

Received 5 January 2021; revised 23 July 2021; editorial decision 26 August 2021; accepted 26 August 2021

The study aims to correlate the effective diameter (D_{eff}) and water-equivalent diameter (D_w) parameters with anterior–posterior (AP), lateral (LAT) and AP + LAT dimensions in order to estimate the patient dose in head CT examinations. Seventy-four patient datasets from head CT examinations were retrospectively collected. The patient's sizes were calculated from the middle slice using a software of IndoseCT. D_w and D_{eff} were plotted as functions of AP, LAT and AP + LAT dimensions. The best trendline fit for LAT and AP functions was a second order polynomial, which resulted in R^2 of 0.89 for D_{eff} vs LAT, 0.88 for D_w vs LAT, 0.92 for D_{eff} vs AP and 0.91 for D_w vs AP. A linear correlation was found for D_{eff} vs AP + LAT, D_w vs AP + LAT and D_w vs D_{eff} with R^2 of 0.97, 0.96 and 0.98, respectively.

INTRODUCTION

Technological improvements in computed tomography (CT) scanners has been increasing rapidly in recent years, especially in terms of the number of detector array, slice number, speed of imaging and image quality[1]. These advances have led to an increased usage of CT scanners[2,3]. Despite being a reliable choice of diagnostic imaging, CT scanners deliver a radiation dose to patients[4,5] and may impose the risk of cancer induction[6,7]. Huang *et al.*[8] found that pediatric head CT examinations were correlated with an increased occurrence of benign brain tumor. Hence, it is important to obtain an accurate dose estimation received by the patients in order to investigate radiation risk caused by CT scanner.

Volume computed tomography dose index ($CTDI_{vol}$) and dose-length product (DLP) displayed on CT scanner consoles are the most extensive metrics as dose indicators. Both metrics are used in the determination of diagnostic reference levels (DRLs)[9]. However, $CTDI_{vol}$ and DLP do not reflect the actual dose received by patients. The patient dose primarily depends on patient size, tissue attenuation and scanner radiation output. $CTDI_{vol}$ was introduced as the standard metric to measure CT output using 16 and 32 cm of cylindrical polymethylmethacrylate (PMMA) reference phantoms, and DLP is the product of $CTDI_{vol}$ and exposure scan length[10]. Hence, neither $CTDI_{vol}$ nor DLP should be considered to assess actual dose received by patients.

The American Association of Physicists in Medicine (AAPM) in report 204 introduced a new metric for estimating dose received by an individual patient and called it as the size-specific dose estimate (SSDE)[11]. SSDE is a simple metric to estimate patient dose on the basis of geometrical size. The basis of geometrical size used in the report 204 is the effective diameter (D_{eff}), i.e. diameter of a circle whose area is the same as the patient cross section. The SSDE is calculated based on a $CTDI_{vol}$ and a size-dependent factor based on the D_{eff}. The D_{eff} was specifically designed for abdomen-pelvic region, which was assumed to be a homogeneous area. The thorax region, which mostly consists of air, will have a higher absorbed dose than the abdomen-pelvic region for the same geometrical size. Hence, a more accurate metric is needed. This problem was solved in AAPM report 220[12] by introducing the water-equivalent diameter (D_w), which considers tissue attenuation. Wang *et al.*[13] found that the use of D_w in calculating the attenuation using CT localizer radiograph gave more accurate results than using only geometry-based (anterior–posterior [AP] and lateral [LAT]) dimensions. This high accuracy was found

especially in the thorax region, although both D_w and geometrical-based calculations gave the proper relationship in the abdomen region.

In AAPM report 204[11], D_{eff} is calculated as the square root of the product of AP and LAT dimensions. However, measuring D_{eff} is sometime cumbersome for busy facilities. Alternatively, D_{eff} can be estimated from the dimensions of AP, LAT or AP + LAT, which are used to determine the size-dependent conversion factor in SSDE calculations. The estimation of D_{eff} through AP, LAT or AP + LAT can be established by the correlations between the two diameters. AAPM report 204 has presented graphs showing the relationships between D_{eff} and AP, D_{eff} and LAT and D_{eff} and AP + LAT for abdominal region. Other regions of the body, such as head, which is one of the frequently subjected studies to CT examinations, are not reported yet[14]. Therefore, the correlation between both AP and LAT dimensions with D_{eff} in head region is interesting to be presented.

As mentioned earlier, D_w is a more robust metric of the patient size to be used to estimate SSDE[15], which can also be calculated from CT localizer radiograph images and axial CT images. Manual measurement of D_w is complicated and requires user intervention to define patient boundaries. However, AAPM recommends an alternative solution to use an automated segmentation to make it more effective. Anam *et al.*[16–18] have developed the IndoseCT software, an automated segmentation-based software, to automatically calculate D_{eff} and D_w. However, to facilitate simpler D_w calculations using LAT and AP, the relationships between LAT and AP to D_w is also necessary to be presented. To the best of our knowledge, the relationships have not been reported yet.

For accurate estimate of the dose at CT head examinations, the AAPM report 293 published the new size-conversion factors[19]. However, AAPM report 293 does not discuss the relationships between LAT, AP, D_{eff} and D_w. The relationships between LAT, AP and D_{eff} are only found at AAPM TG 204 for abdomen and not for the head.

In addition, average D_w from all slices is more accurate than D_w measured at the center slice. The previous study[16] reported that differences of average D_w measured at the center slice are $0.92 \pm 3.37\%$ and $6.75 \pm 1.92\%$ for thorax and head examinations, respectively. This suggests to obtain the average D_w along the longitudinal axis instead of only D_w measured at the center slice. Therefore, the current study aimed to correlate the D_{eff} and D_ws (i.e. average D_w from all slices and D_w measured at the middle slice) parameters with AP and LAT dimensions in order to estimate accurately patient dose in the head CT examination.

METHODS

Datasets

Seventy-four patient datasets were retrospectively taken in DICOM format from January to March, 2019. The datasets were from two scanners, i.e. a 16-slice GE Optima CT520 and a 64-slice Siemens Sensation. The patient ages ranged from 3 days to 79 years old. Pediatric patients were scanned by the 64-slice Siemens Sensations CT scanner with a tube voltage of 120 kVp, tube current of 170 mA, exposure time of 1000 ms and 0.85 pitch. Adult patients were scanned by the 16-slice GE Optima CT520 CT scanner with a tube voltage of 120 kVp, tube current of 298-mA tube, exposure time of 1651 ms, 0.9378 pitch and by the 64-slice Siemens Sensations CT scanner with a tube voltage of 120 kVp, tube current of 297 mA, exposure time of 1000 ms and 0.85 pitch. When head CT examination was performed, the tube current modulation (TCM) was turned off. The patients were scanned in helical mode.

AP, LAT, D_{eff} and D_w calculation

AAPM report 204 reported that AP and LAT dimensions can be measured from CT localizer radiographs and axial CT images using digital calipers[11]. Here, we measured the patient sizes from axial images of head CT examinations. The AP dimension was measured from top side to bottom side of image, and the LAT dimension was measured from the left side to the right side of the body part. Both measurements were performed manually using IndoseCT version 20b as shown in Figure 1. We used the middle slice of the images to evaluate patient sizes.

The automated calculation of D_{eff} has been validated over the phantom and patient images[16]. The D_{eff} value for the head and body phantoms were 15.9 and 31.97 cm, while for patient images show a good correlation compared with manual calculation ($R^2 = 0.996$ in thorax region). There are three options to automatically calculate the D_{eff} using IndoseCT 20b, namely area, center and max. The area option implies that the D_{eff} is calculated directly from the patient cross-sectional area, the center option indicates that the calculation of the diameter is performed using LAT and AP dimension from the center of the image and the max option means that the D_{eff} is calculated based on the LAT and AP dimensions that give the maximum value. We set the automatically calculated D_{eff} based on the area of patients (Figure 2). Anam *et al.*[20] reported that there was no significant difference between calculating the D_{eff} based on area and max options.

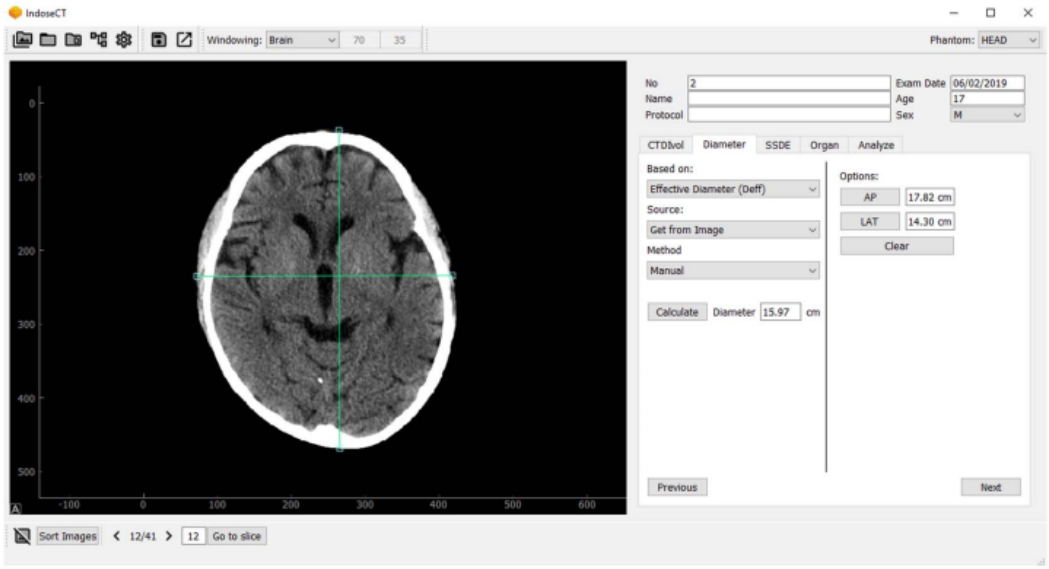

Figure 1. IndoseCT 20b screen display to measure AP dimension and LAT dimension manually.

Equation 1 shows the final calculation to obtain the D_w value[12]:

$$D_w = 2\sqrt{\left[\frac{1}{1000}\overline{HU(x,y)_{ROI}} + 1\right]\frac{A_{ROI}}{\pi}} \quad (1)$$

$\overline{HU(x,y)_{ROI}}$ is the mean CT number in the patient image, which can be determined using measurement tools on the CT workstations or CT console, which requires manual intervention from user. The automatic contour algorithm used in the IndoseCT 20b leads to a more practical alternative approach to obtaining the D_w (Figure 3). In a previous study[14], the algorithm has been verified at the phantom and patient images and provided the D_w value for head phantom of 16.87 cm and body phantom of 33.87 cm. The percentage differences between automatic calculation and manual calculation were <0.5%[14].

AP, LAT, D_{eff} and D_w correlation

AAPM has established D_{eff} as functions of AP, LAT and AP + LAT dimensions to estimate the size-dependent conversion factor. It reported that D_{eff} and AP, D_{eff} and LAT dimensions were correlated through second order polynomial functions (Equation 2) and the sum of AP and LAT was correlated as a linear function to D_{eff} (Equation 3).

$$y = ax^2 + bx + c \quad (2)$$

$$y = ax + b \quad (3)$$

The correlation plots in AAPM report 204 were collected from three different sources of the abdominal region. Here, we used the clinical data from head CT examinations.to find out the correlation and trendline of D_{eff} and D_w.

RESULTS

Figure 4 shows the D_{eff} of head as a function of AP dimension ranging from 10.87 to 19.26 cm. A second order polynomial function is the best-fit trend line in representing the correlation between D_{eff} and AP dimensions. The trend line gives the coefficients a, b, c and R^2, viz. −0.05, 2.41, −10.38 and 0.92, respectively. Figure 5 shows the D_{eff} as a function of LAT dimension ranging from 8.66 to 17.44 cm. The best-fit trendline is a second order polynomial function with a, b and c values of −0.04, 2.06 and −5.23, respectively. The R^2 value is 0.89. The slope of the line decreases as a function of LAT dimension causing a downward curvature in the line. Figure 6 shows the D_{eff} as a function of sum of AP and LAT dimensions. There is a positive linear relationship with a slope of 0.49, an intercept of 0.43 and R^2 is 0.97. The D_{eff}

Figure 2. IndoseCT 20b screen display to automatically calculate D_{eff} based on patient image area.

Figure 3. IndoseCT 20b screen display to automatically calculate D_w from patient's image.

increases as a function of sum of both AP and LAT dimensions.

Figure 7 shows the D_w of head as a function of the AP dimension ranging from 10.87 to 19.26 cm. A second order polynomial function is the best-fit curve with a, b, c and R^2 of −0.06, 2.95, −14.75 and 0.91, respectively. This is similar to the curve of D_w vs AP. Figure 8 shows the D_w as a function of the LAT dimension. The best-fit trendline is a second order polynomial function with a, b and c values of 0.044, 2.30 and − 7.12, respectively, and a R^2 value of 0.88. This R^2 value is almost the same as the R^2 value for the D_{eff} vs LAT curve (0.89). The slope of the line decreases as a function of LAT dimension so it causes a downward curvature of the line. Figure 9 shows the D_w as a function of the sum of AP and LAT

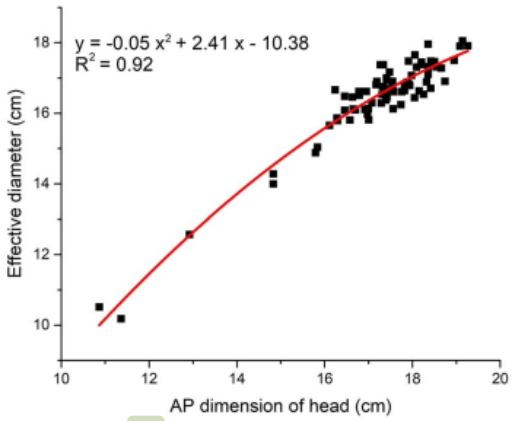

Figure 4. D_{eff} as a function of the AP dimension for head CT examination.

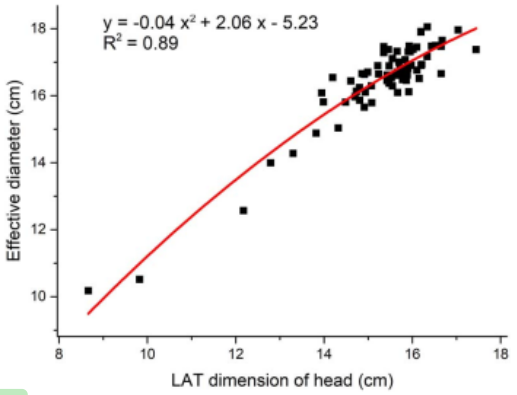

Figure 5. D_{eff} as a function of the LAT dimension for head CT examination.

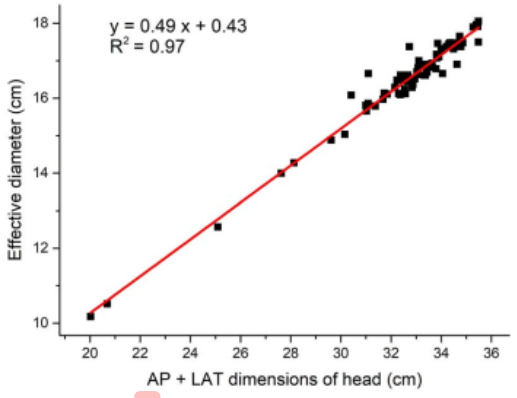

Figure 6. D_{eff} as a function of the sum of AP and LAT dimensions for head CT examination.

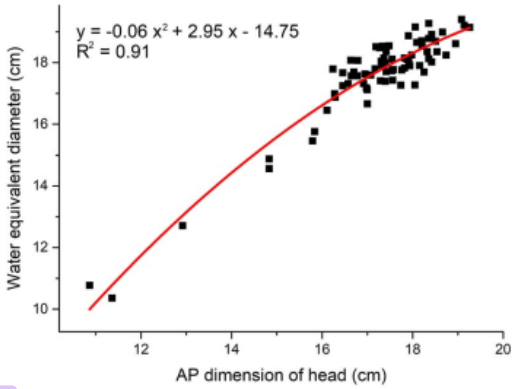

Figure 7. D_w as a function of the AP dimension for head CT examination.

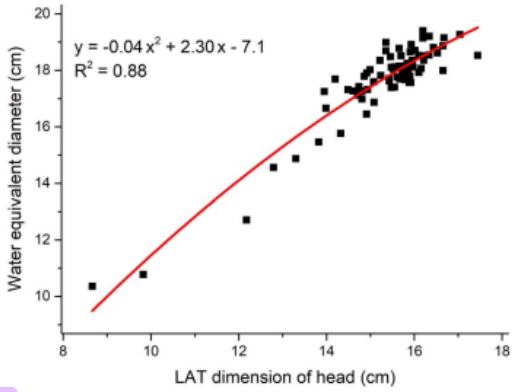

Figure 8. D_w as a function of the LAT dimension for head CT examination.

dimensions. There is a positive linear relationship with a slope of 0.58, an intercept of −1.23 and R^2 of 0.96.

Figure 10 shows the D_w as a function of the D_{eff}. There is a positive linear relationship with a slope of 1.17, intercept of −1.70 and R^2 of 0.98. The D_{eff} increases as the function of the sum of both AP and LAT dimensions. Automatic calculation gives the result value of D_w as 17.6 ± 1.6 cm and D_{eff} as 16.4 ± 1.4 cm.

Figure 11 shows the average D_w of head as a function of the D_w measured at the center. A second order polynomial function is the best-fit curve with a, b, c and R^2 of 0.83, 0.03, −0.16 and 4.5, respectively. It is found that the average D_w of head is 12.8% smaller than the D_w measured at the center. Figure 12 shows the average D_w as a function of the sum of AP and LAT dimensions. There is a positive linear relationship with a slope of 0.56, an intercept of −2.64 and R^2 of 0.77.

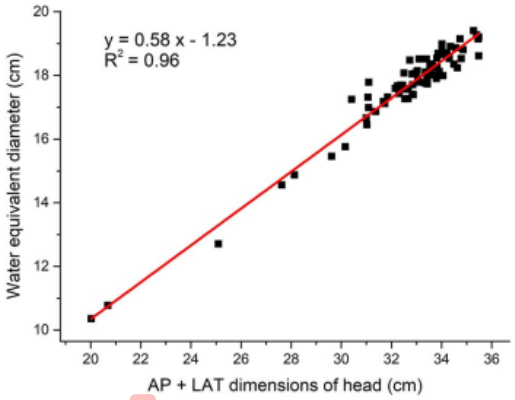

Figure 9. D_w as a function of the sum of AP and LAT dimensions for head CT examination.

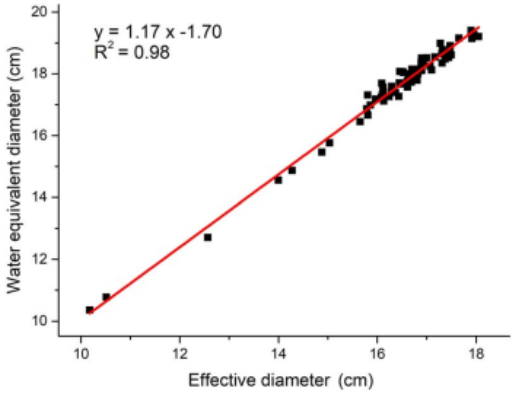

Figure 10. D_w as a function of the D_{eff} for head CT examination.

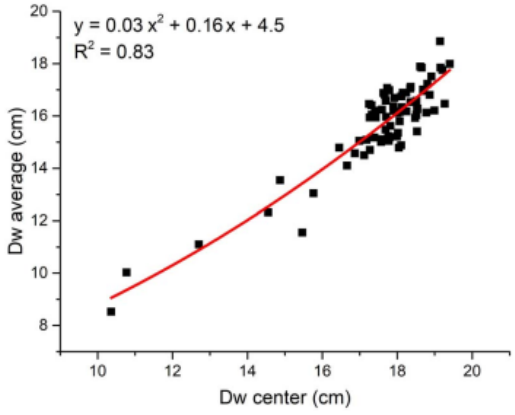

Figure 11. Average D_w as a function of the D_w measured at the center for head CT examination.

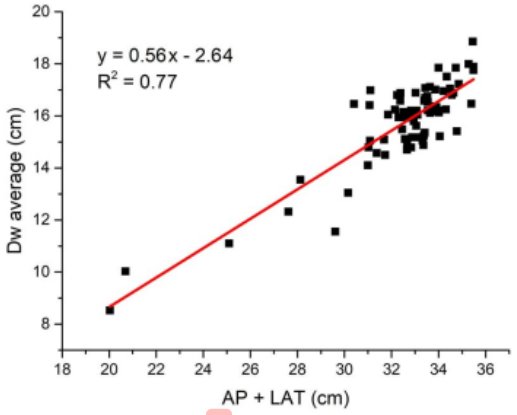

Figure 12. Average D_w as a function of the sum of AP and LAT dimensions for head CT examination.

DISCUSSION

AAPM issued Report 204 to measure pediatric and adult dose from CT examinations as the product of $CTDI_{vol}$ and a size-dependent conversion factor. The size-dependent conversion factor was obtained from four research groups by using physical anthropomorphic phantoms, cylindrical PMMA phantoms, Monte Carlo voxelized phantoms and Monte Carlo mathematical cylinders phantoms. It is expected that using the size-dependent conversion factor will result in more accurate estimate of the patient dose.

The size-dependent conversion factor depends on the phantom diameter[12,13]. The D_{eff} value is calculated as the square root of the product of the AP and LAT dimensions. The AP and LAT dimensions can be measured from a CT localizer radiograph or axial CT image[21,22]. It is very useful in a clinical setting to estimate D_{eff} using one dimension, either AP or LAT. This can be done if relationships between D_{eff} vs AP and D_{eff} vs LAT, have been developed. Plots showing the relationship between D_{eff} vs AP and LAT dimensions were given in Report 204. They show strong correlations between D_{eff} vs AP and D_{eff} vs LAT, with R^2 value of 0.99 for both. However, the correlations were based on the abdominal region only and would need to be found for other body parts.

The plots of D_{eff} as a function of AP and LAT dimensions for head images are shown in Figures 4 and 5. Both plots are second order polynomial functions with a downward curvature. The R^2 value of D_{eff} vs AP is greater than D_{eff} vs LAT. However, there is a difference between the results from our study and the result given in the AAPM Report 204. In the AAPM report, the correlation between D_{eff} vs LAT has a slightly-upward curvature, while our study gives a slightly downward curvature. The AAPM report used data from three different sources i.e. mathematical pediatric phantom, water-equivalent

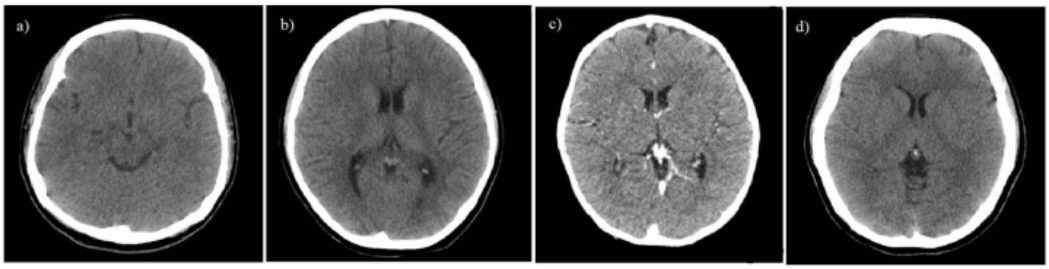

Figure 13. Examples of head images used in this study, (**a**) LAT = 15.92 cm and AP = 16.65 cm, (**b**) LAT = 16.81 cm and AP = 18.21 cm, (**c**) LAT = 12.79 cm and AP = 14.83 cm and (**d**) LAT = 15.7 cm and AP = 17.41 cm.

Table 1. R^2 values and fit parameters between D_{eff} and AP, D_{eff} and LAT, D_{eff} and (AP + LAT), D_w and AP, D_w and LAT, and D_w and (AP + LAT), average D_w and center D_w, and average D_w and (AP + LAT).

Relationship	R^2 Value	*a* Value	*b* Value	*c* Value
D_{eff} vs AP	0.92	−0.05	2.41	−10.38
D_w vs AP	0.91	−0.06	2.95	−14.75
D_{eff} vs LAT	0.89	−0.042	2.06	−5.23
D_w vs LAT	0.88	0.04	2.30	−7.12
D_{eff} vs (AP + LAT)	0.97	0.49	0.43	—
D_w vs (AP + LAT)	0.96	0.58	−1.23	—
D_w vs D_{eff}	0.98	1.17	−1.70	—
Average D_w vs center D_w	0.83	0.03	0.16	4.5
Average D_w vs (AP + LAT)	0.77	0.56	−2.64	—

cylindrical phantom and pediatric patients of CT examinations[23–25] of trunk measurement, whereas we used head clinical data as our source. We believe that the difference in both trendlines is due to the different sources. The head images in our study have a circular or slightly elliptical cross section as shown in Figure 13, which means the AP and LAT values are almost the same. Mean values of AP and LAT dimensions were 17.25 ± 1.47 cm and 15.29 ± 1.36, respectively. We observed the same curvature of D_{eff} vs (AP + LAT dimensions) as the AAPM report, although our R^2 value (0.97) was slightly lower than theirs (1.00). We believe that these small differences are caused by the number of samples used.

We have noted that the essential physical parameter in quantifying X-ray radiation is X-ray attenuation, and one of the factors affecting the attenuation is the object's density in the X-ray pathway. However, the D_{eff} is a metric that is independent of composition. A more suitable metric that incorporates both physical size and composition of the body is the D_w. As we can see from Figure 9, D_{eff} can be used to estimate D_w. To our best knowledge, the correlations between AP dimension, LAT dimension, D_{eff} and D_w for head CT examination has never been reported. These correlations are essential as a primary point to calculate patient dose.

The relationship between the D_{eff} and D_w is shown in Figure 10. From the calculation, we found that the D_w value (17.6 ± 1.6 cm) is slightly higher than D_{eff} (16.43 ± 1.36 cm). Both calculation result is significantly different (p value < 0.05). This is because the main composition of the head is cranium bone and soft tissue. D_w considers both patient's size and composition, but D_{eff} does not. However, there is a linear correlation between both diameters ($R^2 = 0.98$), so that D_{eff} can be confidently used to estimate D_w. A previous study also reported the correlation between D_w and D_{eff}[15,26]. Anam *et al.*[15] reported that D_w also linearly correlated with D_{eff} ($R^2 = 0.73$). Fahmi *et al.*[26] also reported a strong correlation between D_w and D_{eff} ($R^2 = 0.97$).

The relationship between average D_w from all slices is more accurate than D_w measured at the center is shown in Figure 11. From the calculation, we conclude that the average D_w value (15.7 ± 1.8 cm) is slightly smaller than D_w measured at the center (17.6 ± 1.6 cm).

Relationship between AP and LAT dimensions and the average D_w will facilitate easier and more accurate estimates patient size for patient dose estimates. Average D_ws as functions of AP + LAT dimensions are shown in Figures 12.

The best-fit parameters obtained from the current study are summarized in Table 1. In general, D_w correlations were found to be lower than D_{eff}. A recent report compared D_{eff} and D_w values as a function of LAT in the thorax region[27]. It showed the same trend, with the correlation between D_{eff} vs LAT greater than D_w vs LAT[27]. D_{eff} can be determined from $\sqrt{AP \times LAT}$, which does not depend to the body composition.

Our study was based on 74 local patients collected from one hospital in Indonesia. The LAT and AP dimensions were limited from 8.66 to 17.44 cm and 10.87 to 19.26 cm, respectively. It should be noticed that the sample population in our study were predominantly by adult patients and only very small number of pediatric patients. Further studies with the large variations of LAT and AP are needed to confirm the correlation between both dimensions to D_{eff} and D_w. In addition, it is necessary to collect more data from different countries, including from Europeans, Americans and Africans, and to study other body parts, which may have different geometric-size characteristics.

CONCLUSION

The relationships between D_w, D_{eff}, AP, LAT and AP + LAT dimensions of head from 74 local patients have been obtained. The plots of D_w and D_{eff} as a function of AP, LAT and AP + LAT dimensions have similar trendlines. In general, the values of D_{eff} as a function of AP, LAT and AP + LAT dimensions were found to have higher correlations than those of D_w. The plots of D_{eff} were also compared with AAPM 204. All plots, except D_{eff} vs LAT, had similar trends. We believe that the difference was due to the use of different sources between our study and the report published by AAPM. In this study, we also found that the mean value of D_w was higher than the mean value of D_{eff}, because D_w considers geometric size, body composition and attenuation.

ACKNOWLEDGMENTS

This work was funded by the Riset Publikasi International Bereputasi Tinggi (RPIBT), Diponegoro University (contract numbers: 329-116/UN7.6.1/PP/2021).

CONFLICT OF INTERREST

Dr. Choirul Anam and Dr. Geoff Dougherty are IndoseCT developers. This software is not commercially available. It can be made available on request for research purposes. Rest of the authors have no conflicts of interest to disclose.

REFERENCES

1. Romans, L. E. Computed Tomography for Technologists: A Comprehensive Text, (Wolter Kluwer Health) second edn. pp. 1–440 (2011).
2. Bellolio, M. F. *et al. Increased computed tomography utilization in the Emergency Department and its association with hospital admission*. West. J. Emerg. Med. **18**, 835–845 (2017).
3. Pola, A. *et al. Computed tomography use in a large italian region: trend analysis 2004-2014 of emergency and outpatient ct examinations in children and adults*. Eur. Radiol. **28**, 2308–2318 (2018).
4. Smith-Bindman, R. *et al. International variation in radiation dose for computed tomography examinations: prospective cohort study*. BMJ. **364**, 1–12 (2019).
5. Furlow, B. *Radiation dose in computed tomography*. Radiol Technol **81**(5), 437–450 (2010).
6. Brenner, D. J. *Computed tomography – an increasing source of radiation exposure: commentary*. Headache **48**, 657 (2007).
7. Shi, L. and Tashiro, S. *Estimation of the effects of medical diagnostic radiation exposure based on DNA damage*. J .Radiat. Res **59**, 121–129 (2018).
8. Huang, W. Y. *et al. Paediatric head CT scan and subsequent risk of malignancy and benign brain tumour: a nation-wide population-based cohort study*. Br. J. Cancer. **110**, 2354–2360 (2014).
9. Vañó, V., Miller, D. L., Martin, C. J., Rehani, M. M., Kang, K., Rosenstein, M., Ortiz-López, P., Mattsson, S., Padovani, R., and Rogers, A. ICRP Publication 135 Diagnostic Reference Levels in Medical Imaging. Vol. **46**. (ICRP) pp. 1–144 (2017).
10. McCollough, C. H., Leng, S., Yu, L., Cody, D. D., Boone, J. M. and McNitt-Gray, M. F. *CT dose index and patient dose: they are not the same thing*. Radiology. **259**, 311–316 (2011).
11. AAPM. Size-Spesific Dose Estimates (SSDE) in Pediatric and Adult Body CT Examinations. Report of AAPM Task Group 204. (American Association of Physicists in Medicine One Physics Ellipse College Park, MD) pp. 20740–23846 (2011).
12. AAPM. *AAPM TG 220: Use of water equivalent diameter for calculating patient size and size-specific dose estimates (SSDE) in CT*. AAPM Rep **220**, 1–23 (2014).
13. Wang, J., Christner, J. A., Duan, X., Leng, S., Yu, L. and McCollough, C. H. *Attenuation-based estimation of patient size for the purpose of size specific dose estimation in CT. Part II. Implementation on abdomen and thorax phantoms using cross sectional CT images and scanned projection radiograph images*. Med. Phys. **39**, 6772–6778 (2012).
14. Bosch de Basea, M. *et al. Trends and patterns in the use of computed tomography in children and young adults in Catalonia — results from the EPI-CT study*. Pediatr. Radiol **46**, 119–129 (2016).
15. Anam, C., Haryanto, F., Widita, R., Arif, I. and Dougherty, G. *A fully automated calculation of size-specific dose estimates (SSDE) in thoracic and head CT examinations*. J. Phys. Conf. Ser. **694**, 012030 (2016).
16. Anam, C., Haryanto, F., Widita, R., Arif, I. and Dougherty, G. *Automated calculation of water-equivalent diameter (DW) based on AAPM Task Group 220*. J. Appl. Clin. Med. Phys. **17**, 320–333 (2016).

17. Anam, C., Haryanto, F., Widita, R. and Arif, I. *Automated estimation of patient's size from 3D image of patient for size specific dose estimates (SSDE)*. Adv. Sci. Eng. Med. **7**, 892–896 (2015).
18. Anam, C. *et al. An improved method for automated calculation of the water-equivalent diameter for estimating size-specific dose in CT*. J. Appl. Clin. Med. Phys **22**, 313–323 (2021). 10.1002/acm2.13367.
19. AAPM. AAPM TG 293: Size-specific dose estimate (SSDE) for head CT. (American Association of Physicists in Medicine One Physics Ellipse College Park, MD: AAPM Rep No. 293) (2019).
20. Anam, C., Haryanto, F., Widita, R., Arif, I. and Dougherty, G. *The evaluation of the effective diameter (Deff) calculation and its impact on the size-specific dose estimate (SSDE)*. Atom Indonesia. **43**, 55–60 (2017).
21. Pourjabbar, S., Singh, S., Padole, A., Saini, A., Blake, M. A. and Kalra, M. K. *Size-specific dose estimates: localizer or transverse abdominal computed tomography images?* World. J. Radiol. **6**, 210–217 (2014).
22. Brady, S. L. and Kaufman, R. A. *Investigation of American Association of Physicists in medicine report 204 size-specific dose estimates for pediatric CT implementation*. Radiology. **265**, 832–840 (2012).
23. Kleinman, P. L., Strauss, K. J., Zurakowski, D., Buckley, K. S. and Taylor, G. A. *Patient size measured on CT images as a function of age at a tertiary care children's hospital*. Am. J. Roentgenol. **194**, 1611–1619 (2010).
24. Boone, J. M., Cooper, V. N., Nemzek, W. R., McGahan, J. P. and Seibert, J. A. *Monte Carlo assessment of computed tomography dose to tissue adjacent to the scanned volume*. Med. Phys. **27**, 2393–2407 (2000).
25. ICRU. *Patient dosimetry for X rays used in medical imaging*. J. ICRU **5**, 1–113 (2005).
26. Fahmi, A., Anam, C., Suryono and Ali, M. H. *The size-specific dose estimate of paediatric head CT examinations for various protocols*. Radiat. Prot. Dosim **188**, 522–528 (2020).
27. Gabusi, M., Riccardi, L., Aliberti, C., Vio, S. and Paiusco, M. *Radiation dose in chest CT: assessment of size-specific dose estimates based on water-equivalent correction*. Phys. Med. **32**, 393–397 (2016).

Correlation Between Anterior-Posterior and Lateral Dimensions and the Effective and Water-Equivalent Diameters in Axial Images from Head Computed Tomography Examinations

ORIGINALITY REPORT

13%	6%	11%	1%
SIMILARITY INDEX	INTERNET SOURCES	PUBLICATIONS	STUDENT PAPERS

PRIMARY SOURCES

1	Andrew Daudelin, David Medich, Syed Yasir Andrabi, Chris Martel. "Comparison of methods to estimate water-equivalent diameter for calculation of patient dose", Journal of Applied Clinical Medical Physics, 2018 Publication	2%
2	cyberleninka.org Internet Source	1%
3	Or Szekely, Ariel Steiner, Pablo Szekely, Einav Amit, Roi Asor, Carmen Tamburu, Uri Raviv. "The Structure of Ions and Zwitterionic Lipids Regulates the Charge of Dipolar Membranes", Langmuir, 2011 Publication	1%
4	Tomoya Iwaasa, Keiji Tensho, Suguru Koyama, Hiroki Shimodaira, Hiroshi Horiuchi, Naoto Saito, Jun Takahashi. "Clinical outcome of a	1%

	new remnant augmentation technique with anatomical double-bundle anterior cruciate ligament reconstruction: Comparison among remnant preservation, resection, and absent groups", Asia-Pacific Journal of Sports Medicine, Arthroscopy, Rehabilitation and Technology, 2021 Publication	
5	teses.usp.br Internet Source	1 %
6	IFMBE Proceedings, 2009. Publication	<1 %
7	Submitted to University of Sydney Student Paper	<1 %
8	iopscience.iop.org Internet Source	<1 %
9	usir.salford.ac.uk Internet Source	<1 %
10	"Report 87", Journal of the ICRU, 2012. Publication	<1 %
11	M. Gabusi, L. Riccardi, C. Aliberti, S. Vio, M. Paiusco. "Radiation dose in chest CT: Assessment of size-specific dose estimates based on water-equivalent correction", Physica Medica, 2016 Publication	<1 %

12	insights.ovid.com Internet Source	<1%
13	D.Z. Joseph, I.S. Mansur, I. Garba, M.S. Umar, F.B. Nkubli, B. S. Shem. "Diagnostic reference levels for adult's abdominal computed tomography in a referral centre in Nigeria", IOP Conference Series: Earth and Environmental Science, 2021 Publication	<1%
14	Cynthia H. McCollough, Shannon L. McCollough, Justine J. Schneider, Taylor R. Moen et al. "Dependence of Water-equivalent Diameter and Size-specific Dose Estimates on CT Tube Potential", Radiology, 2022 Publication	<1%
15	Andrea Ferrero, Baiyu Chen, Zhoubo Li, Lifeng Yu, Cynthia McCollough. "Technical Note: Insertion of digital lesions in the projection domain for dual-source, dual-energy CT", Medical Physics, 2017 Publication	<1%
16	Dimitris Mihailidis, Virginia Tsapaki, Pelagia Tomara. "A simple manual method to estimate water-equivalent diameter for calculating size-specific dose estimate in chest computed tomography", The British Journal of Radiology, 2020 Publication	<1%

17	Kyle McMillan, Maryam Bostani, Chris Cagnon, Maria Zankl, Ali R. Sepahdari, Michael McNitt-Gray. "Size-specific, scanner-independent organ dose estimates in contiguous axial and helical head CT examinations", Medical Physics, 2014 Publication	<1 %
18	mdpi-res.com Internet Source	<1 %
19	pubs.rsna.org Internet Source	<1 %
20	Achilleas Grigoriadis, Sokratis Mamarikas, Ioannis Ioannidis, Elisa Majamäki, Jukka-Pekka Jalkanen, Leonidas Ntziachristos. "Development of exhaust emission factors for vessels: A review and meta-analysis of available data", Atmospheric Environment: X, 2021 Publication	<1 %
21	Paulo R. Costa, Denise Y. Nersissian, Nancy K. Umisedo, Alejandro H. L. Gonzales, José M. Fernández - Varea. "A comprehensive Monte Carlo study of CT dose metrics proposed by the AAPM Reports 111 and 200", Medical Physics, 2021 Publication	<1 %

22	Supawitoo Sookpeng, Colin John Martin, M R Lopez-Gonzalez. "Simplified approach to estimation of organ absorbed doses for patients undergoing abdomen and pelvis CT examination", Journal of Radiological Protection, 2021 Publication	<1 %
23	www.sciendo.com Internet Source	<1 %
24	Edilaine Honorio da Silva, Oswaldo Baffa, Jorge Elias Jr, Nico Buls. "Conversion factor for SSDE estimation of head CT scans based on age, for individuals from 0 up to 18 years old", Physics in Medicine & Biology, 2021 Publication	<1 %
25	www.neliti.com Internet Source	<1 %
26	www.science.gov Internet Source	<1 %
27	Abdullah Abuhaimed, Colin J Martin, Omer Demirkaya. "Influence of cone beam CT (CBCT) scan parameters on size specific dose estimate (SSDE): a Monte Carlo study", Physics in Medicine & Biology, 2019 Publication	<1 %
28	Christiane Sarah Burton, Annie Malkus, Frank Ranallo, Timothy P. Szczykutowicz. "Technical	<1 %

Note: Model-based magnification/minification correction of patient size surrogates extracted from CT localizers", Medical Physics, 2018
Publication

29 Jyotsana Lal, Bela Farago, Loic Auvray. "Static and Dynamic Perturbations of Droplet Microemulsion by Confinement and Adsorption of Polymer", MRS Proceedings, 2011 — <1%
Publication

30 Medical Radiology, 2012. — <1%
Publication

31 S Sookpeng, C J Martin, M R López-González. "Simplified approach to estimation of organ absorbed doses for patients undergoing abdomen and pelvis CT examination", Journal of Radiological Protection, 2021 — <1%
Publication

Exclude quotes	Off	Exclude matches	Off
Exclude bibliography	On		